



## Estimating individual tree leaf area in loblolly pine plantations using LiDAR-derived measurements of height and crown dimensions

Scott D. Roberts<sup>a,\*</sup>, Thomas J. Dean<sup>b</sup>, David L. Evans<sup>a</sup>, John W. McCombs<sup>c</sup>,  
Richard L. Harrington<sup>a</sup>, Patrick A. Glass<sup>d</sup>

<sup>a</sup> Department of Forestry, and Forest and Wildlife Research Center, Mississippi State University, Box 9681, Mississippi State, MS 39762-9681, USA

<sup>b</sup> School of Renewable Natural Resources, Louisiana State University Agricultural Center, Baton Rouge, LA 70803, USA

<sup>c</sup> NOAA Coastal Services Center, 2234 South Hobson Avenue, Charleston, SC 29405-2413, USA

<sup>d</sup> Mississippi Institute for Forest Inventory, P.O. Box 6350, Starkville, MS 39762, USA

Received 20 September 2004; received in revised form 24 March 2005; accepted 25 March 2005

### Abstract

Accurate estimates of leaf area index (LAI) could provide useful information to forest managers, but due to difficulties in measurement, leaf area is rarely used in decision-making. A reliable approach to remotely estimating LAI would greatly facilitate its use in forest management. This study investigated the potential for using small-footprint LiDAR, a laser-based remote sensing tool capable of characterizing the vertical structure of forest vegetation, to generate estimates of individual tree leaf area based on LiDAR-derived estimates of tree height and crown dimensions. At a 16-year-old loblolly pine spacing trial in Mississippi, LiDAR-derived estimates of leaf area based on height and crown diameter were on average within 0.1 m<sup>2</sup> of ground-based estimates for trees on plots initially planted at a 1.5 m × 1.5 m spacing. For trees on plots originally planted at square spacings of 2.4 m and 3.0 m, LiDAR-based leaf area estimates were below ground-based estimates by 5.8 m<sup>2</sup> and 14.5 m<sup>2</sup>, respectively. At a study site in Texas, LiDAR-derived estimates of leaf area for 4-year-old loblolly pine were, on average, within 0.4 m<sup>2</sup> of ground-based estimates. Errors in leaf area estimates were largely due to the inability to generate accurate LiDAR-based estimates of crown dimensions. Tree heights were accurately estimated with LiDAR at both locations, but crown diameter and vertical crown dimensions at the Mississippi site were underestimated on average by 21% and 3%, respectively.

© 2005 Elsevier B.V. All rights reserved.

**Keywords:** Crown width; Crown depth; Leaf area index; Remote sensing

### 1. Introduction

Forest managers and scientists have long sought efficient ways to estimate leaf area in forested systems. Foliage is the primary site of energy exchange

\* Corresponding author. Tel.: +1 662 325 3044;

fax: +1 662 325 8726.

E-mail address: [sroberts@cfr.msstate.edu](mailto:sroberts@cfr.msstate.edu) (S.D. Roberts).

between trees and the environment; thus, leaf area is fundamentally linked to forest productivity (Gower et al., 1992; McCrady and Jokela, 1998). Accurate estimates of leaf area, either at the stand or at the individual tree level, could provide useful information to forest managers, but due to measurement difficulties, it is rarely used in decision-making.

Existing approaches for directly estimating leaf area index (LAI) of a stand have generally proven too costly, untimely or insensitive to support management decisions. Litterfall collections require several months and are generally impractical for management purposes. Allometric equations are often used to estimate leaf area of individual trees, which are then summed across an area to estimate LAI. These equations are expensive to develop and may not apply across wide ranges of sites (Whitehead, 1978; Shelburne et al., 1993). In addition, they require collection of considerable amounts of field data for their application:

Due to difficulties and expense of attaining direct estimates of LAI from traditional approaches, considerable efforts have been made over the past quarter century to develop techniques to indirectly estimate LAI using remote sensing technologies. Vegetation indices derived from satellite images have been significantly correlated to LAI in a wide range of forest types (Spanner et al., 1994; Wulder et al., 1996; Fassnacht et al., 1997). However, several factors introduce error into satellite-based estimates of LAI, based on spectral reflectance.

Continued advances in remote sensing technology are leading to improvements in data generated by satellite-based and other aerial-based platforms, thus enhancing capabilities to estimate forest conditions across large land areas. Newer platforms are capable of finer spatial and spectral resolutions, and new analytical techniques allow increasingly detailed information to be extracted from remotely sensed data (Wu and Strahler, 1994; Wulder et al., 1998). In spite of these improvements, the ability to remotely sense forest structural characteristics, including LAI, with current satellite and aerial-based spectral tools remain limited (Wulder et al., 1998; Holmgren and Thuresson, 1998), due largely to the inability of spectral imagery to adequately characterize the vertical structure of forest canopies (Hall et al., 2005).

Ground-based remote sensing tools are also available for estimation of LAI using approaches based on the penetration of light through the canopy. Estimates of LAI from ground-based sensors, however, while correlated with direct estimates, are often biased (Gower and Norman, 1991; Fassnacht et al., 1994). Ground-based tools currently are incapable of consistently providing accurate estimates of LAI or are limited by the need for species- or site-specific coefficients or correction factors. In addition, the number of sampling points per stand required to estimate LAI with acceptable precision is time consuming and does not easily lend itself to measurements over large land bases.

The past decade has seen increasing interest in the use of light detection and ranging (LiDAR) technologies in forestry applications. LiDAR systems measure the time required for a pulse of laser energy emitted from an aircraft to reflect, or 'echo', off surfaces. Time is converted to distance, and through post-processing procedures, these distances provide a sampling of the vertical distribution of the vegetation canopy. The most commonly used LiDAR systems in forest applications are small-footprint, scanning systems. These systems operate by scanning side-to-side while emitting laser pulses resulting in a swath of laser postings through the stand. The width of the swath is determined by the scan angle and the aircraft altitude. The diameter of the footprint of laser energy when it reaches the surface is generally between 0.1 m and 1.0 m. Existing systems are often capable of generating in excess of 4 posts  $m^{-2}$ , although posting densities of 1–2  $m^{-2}$  or lower are more common.

Studies using small-footprint LiDAR to assess forest conditions have typically attempted to estimate average stand conditions (e.g., mean height, average dominant height, stem density, basal area, standing volume, aboveground biomass, foliage biomass) (Hall et al., 2005; Magnussen and Boudewyn, 1998; Means et al., 2000; Næsset, 1997a,b, 2002; Næsset and Bjercknes, 2001). The most common approach has been to derive various statistical metrics directly from the LiDAR data. These metrics are then included as independent variables in regression analyses that examine correlations with measured stand data. While some of these analyses have resulted in reasonable correlations, the relationships are generally site

specific and of limited use in predicting stand values elsewhere.

Improvements in LiDAR technology have led to higher pulse rates and increased LiDAR posting densities, thus making LiDAR analysis of individual tree characteristics possible. One approach to individual tree analysis, as with stand-level analysis, is to correlate tree and crown dimensions with statistical metrics derived from the LiDAR data using regression techniques (Næsset and Økland, 2002). This approach has generally been attempted on relatively large, open-grown trees—not in closed canopy forests. A more direct approach to individual tree analysis involves interpolation of the LiDAR returns emanating from the canopy into a canopy surface model. Peaks in the surface model are identified as trees. This approach has been used to identify individual trees (Andersen et al., 2001; McCombs et al., 2003), and to estimate tree heights (Hyypä and Inkinen, 1999; McCombs et al., 2003; Popescu and Wynne, 2004) and crown diameters (Popescu et al., 2003). Attempts have also been made to use LiDAR-derived individual tree information to derive stem diameters and basal area (Hyypä and Inkinen, 1999; Hyypä et al., 2001), and to estimate stand-level volume and biomass (Popescu et al., 2004).

The success of these efforts has shown that LiDAR is capable of providing structural information at the individual tree level. Roberts et al. (2003) show that individual tree leaf area is reasonably estimated from crown dimensions; which suggests that LiDAR may be capable of providing estimates of individual tree leaf area. If individual tree leaf areas can be estimated with suitable accuracy, then LiDAR may be capable of providing stand-level estimates of leaf area capable of supporting management decisions.

Our goal in this study was to estimate individual tree leaf area using estimates of tree and crown dimensions derived from LiDAR. Our first objective therefore was to evaluate the ability of LiDAR to accurately recover stem and crown dimensions that are used in estimating leaf area. Accuracy was assessed by comparing LiDAR-derived estimates of tree dimensions with ground-based measurements for trees accurately identified with LiDAR. Our second objective was to evaluate the accuracy of LiDAR-based estimates of individual tree leaf area derived from LiDAR-based estimates of stem and crown

dimensions. LiDAR-based leaf area estimates were compared to estimates of leaf area derived from ground-measured data.

## 2. Methods and materials

### 2.1. Study sites

Loblolly pine plantations located in east-central Mississippi and eastern Texas were used in this study. In Mississippi, the Starr site utilized a 16-year-old loblolly pine spacing trial located on the Mississippi State University Starr Memorial Forest (33°16'N, 88°52'W) (Land et al., 1991). The original study included eight replicates of three intertree spacings—1.5 m × 1.5 m (4305 trees ha<sup>-1</sup>), 2.4 m × 2.4 m (1682 trees ha<sup>-1</sup>) and 3.0 m × 3.0 m (1076 trees ha<sup>-1</sup>). Each spacing block within each replicate contained eight, 12.2 m × 12.2 m measurement plots. Limitations in the availability of LiDAR data restricted us to using 21 of the 1.5 m spacing plots, 13 of the 2.4 m spacing plots and 14 of the 3.0 m spacing plots. Current tree density on the 48 plots averaged 2401, 1075 and 801 trees ha<sup>-1</sup>, respectively, for the three initial spacings. Planting on exact spacing provided information on the precise location of every live tree within each plot.

In Texas, the Fred site utilized a 4-year-old loblolly pine long-term site productivity study located in Tyler County near Fred, TX (30.6°N, 94.4°W) (Carter et al., 2002). The study was laid out in a randomized complete-block design with factorial combinations of two levels of harvest disturbance (high and low), bedding (presence or absence) and fertilization (presence or absence). The eight treatments were randomly assigned to 0.12-ha treatment plots within each of three blocks. The previous mature stand was harvested in summer 1994, and the bedding treatment applied in October 1994. Herbicides were broadcast across the entire site in September 1994 and again in September 1995. Following extensive mortality in the original 1995 planting, the site was replanted in February 1996 at a spacing of 2.0 m × 3.0 m. Fertilized plots received 250 kg ha<sup>-1</sup> of diammonium phosphate, broadcast by hand, in May 1996. Measurement plots of 10 rows × 10 trees were contained within the treatment plots.

## 2.2. Data

### 2.2.1. Standing trees

At the Starr site, all trees on each measurement plot were measured in March 2001. Measurements included diameter at breast height (DBH, 1.37 m), total tree height (HT), height to base of live crown ( $HT_{\text{blc}}$ ), and crown radius in the four cardinal directions. At the Fred site, measurements taken in January 2001 included total tree height on all trees existing within the  $10 \times 10$  tree measurement plot. Within a  $5 \times 4$ -tree subplot established at the center of each measurement plot, stem diameter,  $HT_{\text{blc}}$ , and crown diameter along and across rows were measured for all trees.

Estimates of height to crown center ( $HT_{\text{mc}}$ ), defined as the height to the median in leaf area, were derived from field measurements of each tree at the Starr site. The distribution of leaf area in destructively harvested trees indicated that this height generally occurred at the vertical midpoint of the crown. Consequently, height to crown center was calculated as  $(HT_{\text{blc}} + HT)/2$ .

A summary of the field data for the variables used in this analysis is given in Table 1. Field data from both sites were linked to a GIS layer identifying the relative location of each tree on each plot. Knowing the precise location of each live tree allowed tree-to-tree comparison of LiDAR-based estimates of tree and crown dimensions with ground measurements.

### 2.2.2. Destructive data

Selected trees at both study sites were destructively sampled in order to develop equations for calculating individual tree leaf area from both ground-based tree measurements and LiDAR-derived estimates of tree dimensions. At the Starr site, 65 trees from seven, half-sib families and an unimproved check were destructively harvested in August 1999. At the Fred site, 49 trees were destructively sampled in August 2000. Details of the sampling procedures at each location are contained in Roberts et al. (2003) and Dean et al. (2002), respectively. In brief, trees were felled and separated into their main components (stem, branches and foliage). Each component was weighed fresh, and a subsample was returned to the laboratory for further analyses that allowed determination of total dry weight of each component, and total crown leaf area. These data provided the basis for evaluating regression models estimating leaf area from stem diameter, total tree height, crown length, height to crown center and crown diameter.

### 2.2.3. LiDAR data

LiDAR data were collected for both sites on 19–20 October 2000. Data were acquired using an Optech ALTM 1210 system, and included information on first and last returns. System parameters for the data collection are provided in Table 2. A relatively low flying altitude and narrow scan angle were required to achieve the high posting densities needed for individual tree analysis. A posting density of 4–5 posts  $\text{m}^{-2}$

Table 1  
Descriptive statistics for measured or estimated field values for all live trees on plots at the Starr (Mississippi) and Fred (Texas) sites

	DBH (cm)	Height (m)	Crown diameter (m)	Height to crown center (m)	Estimated leaf area <sup>a</sup> ( $\text{m}^2$ )
Starr site					
Mean	6.7	17.5	3.0	14.7	24.6
Minimum	3.5	8.6	0.9	7.2	5.0
Maximum	12.5	21.2	7.5	17.6	108.4
S.D.	1.7	1.6	1.1	1.1	15.7
<i>n</i>	1008	1007	998	1003	1003
Fred site					
Mean	6.5	4.7	2.1	2.9	14.8
Minimum	0.4	0.4	0.4	0.3	0.03
Maximum	12.2	7.7	3.7	5.3	46.4
S.D.	2.3	1.2	0.6	0.7	8.6
<i>n</i>	379	1922	382	382	1922

DBH and crown diameter were subsampled at the Fred site. Differing *n* values at the Starr site due to missing or unusable data.

<sup>a</sup> Estimated leaf areas are based on allometric equations developed from destructively sampled trees at each location.

Table 2

System and mission parameters for the LiDAR data collection mission for the Starr (Mississippi) and Fred (Texas) study sites, 19–20 October 2000

Parameter	Specification
LiDAR system	Optech ALTM 1210
Laser pulse frequency (kHz)	10
Mirror scan angle	$\pm 3^\circ$ off nadir
Mirror scan frequency (Hz)	65
Aircraft altitude (m)	$\sim 360$
Vertical accuracy (m)	0.15
Horizontal accuracy (m)	0.40
Beam divergence (mrad)	0.30
Nominal footprint diameter (m)	0.11
Data collected	First/last return; intensity

was achieved within individual flight lines. To increase the density of the LiDAR data, returns from overlapping flight lines were combined. Swath widths of individual flight lines averaged ca. 40 m, with an attempted 30–40% overlap between adjacent swaths. Due to the narrow swaths required to meet demanding mission parameters, the degree of overlap was variable. Resulting posting densities varied from 4 posts  $m^{-2}$  to 20 posts  $m^{-2}$  at the Starr site and from 6 posts  $m^{-2}$  to 10 posts  $m^{-2}$  at the Fred site.

### 2.3. LiDAR analytical procedures

#### 2.3.1. Tree identification and height estimation

The procedures used to identify locations and estimate heights of individual trees are detailed in McCombs et al. (2003). A ground surface model was created through interpolation of the last return LiDAR data points. An iterative filtering approach was used to remove data points not reflected from the ground surface (McCombs et al., 2003). Linear interpolation procedures in ERDAS Imagine (Version 8.4, Erdas Inc., Atlanta, GA) were used to create a surface grid model with a grid cell size of ca. 0.15 m. First return LiDAR data points were used to create a canopy surface model, again using linear interpolation and a grid cell size of ca. 0.15 m. This cell size was chosen to accurately represent surface variations while preserving the integrity of the original LiDAR data by minimizing the occurrence of cells with multiple LiDAR returns.

The location of individual trees was determined by assuming the pixel associated with the peak of a tree

will be higher than surrounding pixels within the canopy surface model. A pixel was deemed a crown peak if, as the center pixel, it was higher than all neighboring pixels within a circular focal search window. The search window radius was chosen so that if the window were centered on a tree peak only one tree would fall within the window. At the Starr site, the radius was 0.76 m in the 1.5 m plot spacing and 1.2 m in the 2.4 m and 3.0 m plot spacings. At the Fred site, the search window radius was 0.914 m. The height of each identified tree was calculated by subtracting the pixel elevation value of the LiDAR ground surface from the pixel elevation value of the LiDAR canopy surface at each identified tree peak location.

Tree identification accuracy is important since estimates of leaf area and physical dimensions of individual trees identified with LiDAR will ultimately be used to calculate mean tree characteristics at the stand-level. In this study, accurately identified trees were those where a peak in the canopy surface model could be tied directly to a known live tree on the ground. LiDAR fails to detect some live trees (omission errors), and incorrectly identifies some peaks in the canopy surface model as live trees (commission errors) (McCombs et al., 2003). We were therefore able to compare the characteristics of the accurately identified trees with those of all peaks identified as trees, and to the “true” population of trees on the ground. We also assessed net identification accuracy, defined as the total number of trees identified in the canopy surface model (including commission errors) relative to the total number of live trees known to exist on the ground.

#### 2.3.2. Estimation of crown dimensions

LiDAR data from the Starr site were used in an attempt to locate the base of the canopy. A canopy base layer was determined by passing a focal search window over the canopy surface layer to generate a set of local minimum pixel values. These values were interpolated into a new grid surface layer. While most of these values were from near the base of the canopy, some of the pixel values originated from canopy gaps and were from near the ground surface. Therefore, a second search window was passed over this surface layer, this time retaining local maximum pixel values. To further ensure that no values were reflected from

the ground or ground-layer vegetation, all pixel values less than 5 m in height were automatically filtered out since the minimum height to the base of the live crown exceeded 5 m. The remaining pixel values were interpolated into a surface representing the base of the canopy.

LiDAR-based estimates of crown diameter ( $CD_{lid}$ ) were determined by locating the crown edge in each cardinal direction from identified tree peaks in the canopy surface layer. A linear array of cells from the canopy surface model was extended out 3.4 m in each cardinal direction from each identified tree peak. A search algorithm was written within the ERDAS Imagine software which identified the minimum pixel elevation value in the array, and identified that as the “saddle” formed between adjacent crowns in the canopy surface model. The location of the pixel was assumed to represent the crown edge. Given that crowns of adjacent trees do not commonly overlap in loblolly pine, we felt this was a reasonable assumption. Where gaps occurred between crowns, the location of the crown edge was assumed where the elevation of the linear array fell below that of the canopy base layer. A crown radius was determined as the distance from the tree peak to each of the four identified crown edges. Crown diameter was calculated as twice the average of the four radii.

The location within an individual crown that is associated with the median leaf area has not been correlated with any specific morphological feature of the crown. Since solar radiation rapidly attenuates in the canopy once crowns form a relatively continuous canopy layer, height to crown center was assumed to correspond with the height where crowns of adjacent trees met. Data presented by Sinclair and Knoerr (1982) for a 15-year-old loblolly pine plantation also suggest that the point where crowns meet and form a continuous canopy corresponds with the center of leaf area distribution. In the LiDAR-derived canopy surface model, a saddle is formed at the point where two crowns come together. For each tree, the pixels located in these saddles were identified, and their elevation values were averaged to get an estimated height to the crown center ( $CC_{lid}$ ).

### 2.3.3. Estimation of leaf area

Equations for calculating leaf area from both ground- and LiDAR-based tree dimensions were

developed with nonlinear regression models of the form

$$Y = b_0 X_1^{b_1} X_2^{b_2},$$

where  $Y$  is leaf area per tree,  $X_1$  and  $X_2$  are stem or crown dimensions and  $b_0$ – $b_2$  are regression coefficients. Selection of the models used to calculate leaf area was based on three criteria: (1) accuracy and precision of the leaf area estimates as indicated by residual plots and the fit index (FI); (2) reliability of the LiDAR-based estimates of tree or crown dimensions used as independent variables in the prediction equations; and (3) agreement between conventional ground-based estimates of leaf area and estimates based on ground measurement of the tree and crown dimensions derived from LiDAR for leaf area estimation. For the Starr site, the set of equations that met our modeling criteria were

$$LA_1 = \frac{0.1216 DBH^{2.4422}}{HT_{mc}^{0.6610}} \quad (1)$$

$$(n = 103, s_y = 0.47 \text{ m}^2, \text{ FI} = 0.61, \text{ weighted by inverse of } DBH^2);$$

$$LA_2 = 0.0068 HT^{2.7993} CD^{0.4405} \quad (2)$$

$$(n = 102, s_y = 1.12 \text{ m}^2, \text{ FI} = 0.75, \text{ weighted by inverse of } HT^2);$$

and

$$LA_3 = \frac{0.0007 HT^{7.1342}}{HT_{mc}^{3.8145}} \quad (3)$$

$$(n = 103, s_y = 0.94 \text{ m}^2, \text{ FI} = 0.82, \text{ weighted by inverse of } HT^2).$$

Eq. (1) was used to calculate leaf area from ground-based measurements. Eqs. (2) and (3), while developed from ground-based measurements of destructively harvested trees, were used to estimate leaf area from LiDAR-derived estimates of tree height and either crown diameter or height to crown center. Comparisons of leaf area estimates derived from Eq. (1) to estimates derived from Eqs. (2) and (3) yielded the following results:

$$LA_1 = 0.510 + 0.994 LA_2 \quad (r^2 = 0.76)$$

and

$$LA_1 = -0.634 + 1.014LA_3 \quad (r^2 = 0.90).$$

Analysis of the destructive harvest data at the Fred site showed that tree height was the best predictor of individual tree leaf area. The equation used to calculate leaf area of trees at the Fred site from both ground-based measurement and LiDAR-based estimation of tree heights was

$$LA = 0.2720HT^{2.5178}$$

( $n = 48$ ,  $s_f = 1.25 \text{ m}^2$ , FI = 0.87, weighted by residual variance).

#### 2.4. Statistical analysis

Covariance between LiDAR- and ground-based measurements of leaf area and associated variables was examined with simple linear regression to test the null hypothesis that the slope between the variables was equal to one. Simple differences between LiDAR- and ground-based measurements were tested with paired *t*-tests to test the hypothesis that measurements made with LiDAR were equal to measurements made with conventional ground procedures. The effects of initial spacing and regeneration practices on measured values and paired differences between LiDAR- and ground-based measurements were tested with analysis

of variance techniques using one-way designs for the Starr site and randomized complete-block designs with  $2 \times 2 \times 2$  factorial treatments for the Fred site.

### 3. Results

#### 3.1. Tree identification accuracy

Across all initial tree spacings, an average of 81% of all live loblolly pine trees were accurately identified on plots at the Starr site (Table 3). Initial spacing significantly affected the ability to identify live trees ( $F_{2,45} = 90.6$ ,  $P < 0.0001$ ). The accuracy of live tree identification was 68.1% on the 1.5 m plots, 88.8% on the 2.4 m plots and 93.1% on the 3.0 m plots. Commission error rates ranged from 4.9% on the 2.4 m plots to 9.9% on the 3.0 m plots, although these differences were not significant ( $F_{2,45} = -1.97$ ,  $P = 0.152$ ). Net identification accuracy, which includes accurately identified trees plus commission errors, was 89.0% overall—76.7% on the 1.5 m plots, 93.8% on the 2.4 m plots and 103.0% on the 3.0 m plots.

At the Fred site, nearly 70% of live trees were accurately identified (Table 3). Bedding was the only treatment that significantly affected identification accuracy ( $F_{1,14} = 5.96$ ,  $P = 0.029$ ). On bedded plots, 74.2% of the trees were accurately identified, while on unbedded plots only 65.7% of live trees were located.

Table 3

LiDAR tree identification accuracy for different initial tree spacings at the Starr site in Mississippi, and for different site preparation treatments at the Fred site in Texas

Spacing	Starr site					
	Number of plots	Average number live trees per plot	Percent live trees accurately identified	Commission errors as percent of live trees <sup>a</sup>	Net identification accuracy <sup>b</sup>	
1.5 m × 1.5 m	21	36.0	68.1	8.6	76.7	
2.4 m × 2.4 m	13	16.1	88.8	4.9	93.8	
3.0 m × 3.0 m	14	12.6	93.1	9.9	103.0	
All MS plots	48		81.0	8.0	89.0	
Treatment	Fred site					
	Bedded plots	12	75.3	74.2	16.7	90.9
	Unbedded plots	12	74.8	65.7	18.6	84.3
	All TX plots	24		69.9	17.7	87.6

<sup>a</sup> Commission errors include trees double counted, standing dead trees that generated a peak in the interpolated LiDAR canopy surface model, and peaks in the LiDAR canopy model of unknown cause.

<sup>b</sup> Net identification accuracy is the number of accurately identified trees plus the number of commission errors divided by the actual number of live trees on a plot.

The average commission error rate (17.7%) did not differ significantly among treatments. Net identification accuracy averaged 87.6%, again varying significantly ( $F_{1,14} = 4.71$ ,  $P = 0.048$ ) between bedded (90.0%) and unbedded (84.3%) plots.

### 3.2. Tree height estimation

The average ground-measured height of trees correctly identified by LiDAR on the Starr site was 18.0 m, compared to an average LiDAR-estimated height of 17.5 m (Table 4). The average difference of 0.5 m was significant ( $t_{n=864} = -28.6$ ,  $P < 0.001$ ). Regression analysis between  $HT_{gnd}$  and  $HT_{lid}$  found a strong linear correlation with a slope of nearly 1.0 ( $HT_{gnd} = 0.508 + 0.997HT_{lid}$ ,  $n = 864$ ,  $s_y = 0.5$  m,  $r^2 = 0.84$ ), suggesting that the mean difference represents a consistent bias (Fig. 1a).

The average ground-measured height for all live trees at the Starr site was 17.5 m (Table 4), while the average height of trees missed by LiDAR was only 15.5 m, indicating that LiDAR had difficulty detecting shorter than average trees. The average LiDAR-estimated height of commission error trees was 1.1 m shorter than accurately identified trees (16.4 m versus 17.5 m), indicating that trees “created” by LiDAR were also shorter than average.

There was no statistically significant spacing effect on either the slope ( $F_{2,858} = 0.38$ ,  $P = 0.632$ ) or the intercept ( $F_{2,858} = 0.46$ ,  $P = 0.686$ ) of the simple linear regression between field-measured and LiDAR-estimated tree heights of accurately identified trees. LiDAR-based height estimates were correlated with field-measured heights with similar precision across

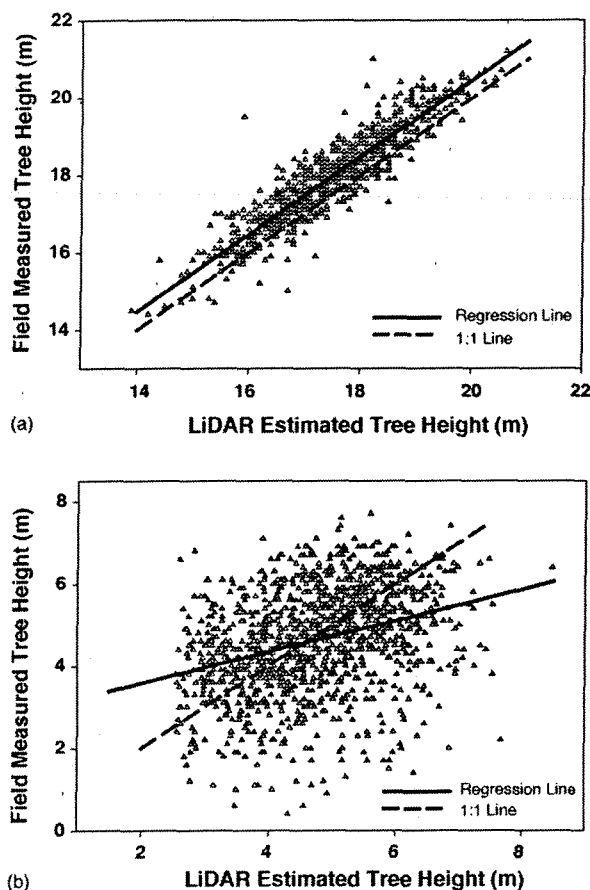


Fig. 1. Field-measured vs. LiDAR-estimated tree heights for correctly identified trees at the (a) Starr site in Mississippi (regression relationship:  $HT_{gnd} = 0.508 + 0.997HT_{lid}$ ,  $n = 864$ ,  $r^2 = 0.84$ ,  $RMSE = 0.48$  m) and (b) Fred site in Texas (regression relationship:  $HT_{gnd} = 2.8198 + 0.3809HT_{lid}$ ,  $n = 1270$ ,  $r^2 = 0.11$ ,  $RMSE = 1.18$  m).

Table 4  
LiDAR-derived versus ground-based estimates of tree heights and crown dimensions at the Starr site (Mississippi) and the Fred site (Texas)

Category	Height (m)				Crown diameter (m)				Crown center (m)	
	Starr site		Fred site		Starr site		Fred site		Starr site	
	LiDAR	Ground	LiDAR	Ground	LiDAR	Ground	LiDAR	Ground	LiDAR	Ground
Correct ID trees	17.5 (1.1)	18.0 (1.2)	4.8 (1.1)	4.6 (1.3)	2.7 (0.7)	3.4 (1.1)	5.5 (1.2)	2.1 (0.6)	14.5 (1.0)	14.9 (0.9)
All live trees		17.5 (1.6)		4.7 (1.2)		3.0 (1.1)		2.1 (0.6)		14.7 (1.1)
All LiDAR trees	17.4 (1.2)		4.8 (1.1)		2.6 (0.7)		5.5 (1.2)		14.4 (1.1)	
Omitted trees		15.5 (1.5)		4.7 (1.2)		2.3 (0.8)		2.1 (0.6)		13.4 (1.3)
Committed trees	16.4 (1.5)		4.8 (1.1)		2.0 (0.8)		6.9 (0.9)		13.8 (1.6)	

Ground-based values are means for all existing trees at each study site, including those not identified (omission errors) with LiDAR. LiDAR-derived values are means for all trees identified using interpolated LiDAR data, including nonexistent trees (commission errors) identified from LiDAR. Standard deviations are in parentheses.

all three spacings. The 2.4 m spacing plots had the tightest relationship ( $r^2 = 0.89$ ,  $s_y = 0.4$  m). The precision of the 3.0 m spacing plots ( $r^2 = 0.88$ ,  $s_y = 0.4$  m) was similar to the 2.4 m plots, while the 1.5 m spacing plots were most variable ( $r^2 = 0.77$ ,  $s_y = 0.5$  m).

At the Fred site, the average difference between  $HT_{lid}$  and  $HT_{gnd}$  of correctly identified trees was +0.2 m (Table 4), which was significantly different from zero ( $t_{n=1270} = 3.23$ ,  $P = 0.001$ ). In this case, however, the difference cannot be considered a bias. The correlation between ground-measured and LiDAR-estimated individual tree heights was weak, and the slope of the relationship differed substantially from 1.0 ( $HT_{gnd} = 2.82 + 0.381HT_{lid}$ ,  $n = 1270$ ,  $r^2 = 0.11$ ,  $s_y = 1.2$  m) (Fig. 1b). There were no significant treatment effects on the difference between LiDAR- and ground-based measurements of height ( $F_{1,14} < 0.36$ ).

The average ground-measured height for all trees at the Fred site was 4.7 m (Table 4)—0.1 m taller than the mean height of the trees correctly identified with LiDAR. The average  $HT_{lid}$  of the commission error trees was 4.8 m, equal to the height of the correctly identified trees. Omission error trees averaged 4.7 m in height, 0.1 m taller than the average for correctly identified trees. Unlike the Starr site, there was not a tendency for LiDAR to miss shorter than average trees at the Fred site. Commission error trees were slightly taller, on average, than the actual heights of trees in the stand. In some cases, this may have been due to LiDAR detecting competing vegetation that was taller than the adjacent trees.

### 3.3. Crown diameter estimation

The average ground-measured crown diameter (CD) for correctly identified trees at the Starr site was 3.4 m compared to an average LiDAR-estimated CD of 2.7 m (Table 4). A simple linear relationship between ground- and LiDAR-based crown diameters was significant ( $CD_{gnd} = 0.26 + 1.17 CD_{lid}$ ,  $n = 855$ ,  $r^2 = 0.55$ ) (Fig. 2); however, the average underestimation by LiDAR of 0.7 m (which was significantly different from zero ( $t_{n=855} = 27.0$ ,  $P < 0.0001$ )) cannot be considered a consistent bias since the average error was not equal to the intercept in the simple linear equation correlating  $CD_{gnd}$  to  $CD_{lid}$ .

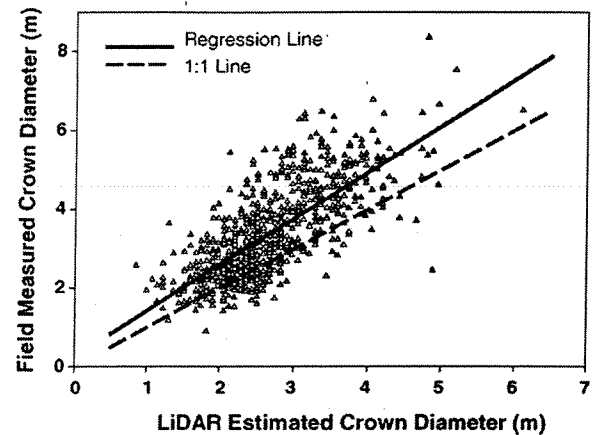


Fig. 2. Field-measured vs. LiDAR-estimated crown diameters for correctly identified trees at the Starr site in Mississippi (regression relationship:  $CD_{gnd} = 0.26 + 1.17CD_{lid}$ ,  $n = 855$ ,  $r^2 = 0.55$ ).

$CD_{gnd}$  of all live trees on the plots averaged 3.0 m.  $CD_{gnd}$  of trees missed by LiDAR averaged nearly 0.9 m less than that of trees accurately identified. The average  $CD_{lid}$  of commission error trees was only 2.0 m. As with tree heights, crown diameters of both omitted and committed trees were considerably smaller than those of correctly identified trees at the Starr site.

As expected, there was a significant spacing effect on crown diameter—trees at wider spacing had, on average, wider crowns. There was also a spacing difference in how well LiDAR was able to estimate crown diameters. For trees on the 1.5 m, 2.4 m and 3.0 m spacing plots, LiDAR underestimated CD by an average of 0.46 m, 0.93 m and 1.25 m, respectively. Regression relationships also showed that LiDAR-based estimates of crown diameters on the 1.5 m spacing plots ( $s_y = 0.56$  m) were more precise than both the 2.4 m plots ( $s_y = 0.72$  m) and the 3.0 m plots ( $s_y = 0.94$  m).

No significant correlation was found between ground-measured and LiDAR-estimated crown diameter for trees at the Fred site ( $P = 0.610$ ). The relative error of LiDAR-based estimates was over 200% (Table 4). This large error reflects our technique of identifying crown edges by attempting to locate the saddle created by adjacent interacting crowns. In these 4-year-old stands, where the canopies had not yet reached closure and individual crowns had not yet begun to recede, our approach simply located a middle

distance between individual trees, thus greatly overestimating crown diameters.

### 3.4. Height to crown center estimation

The average LiDAR-based estimate of height to crown center ( $CC_{lid}$ ) for correctly identified trees at the Starr site was 14.5 m. This differed from the average ground-measured height to crown center ( $CC_{gnd}$ ) by 0.4 m, although this difference was not significant ( $t_n = 855 = 1.30, P = 0.192$ ) (Table 4). Again, given the slope and intercept values of the simple linear regression, this underestimation cannot be considered a consistent bias ( $CC_{gnd} = 6.78 + 0.56CC_{lid}, n = 846, r^2 = 0.40$ ) (Fig. 3).

The average  $CC_{gnd}$  of all live trees on the plots averaged 14.7 m, 0.2 m greater than the average LiDAR-based estimate for correctly identified trees.  $CC_{gnd}$  of missed trees averaged 1.5 m smaller than that of correctly identified trees.  $CC_{lid}$  of commission error trees was 0.6 m smaller than the average for all LiDAR-identified trees.

There were no significant spacing effects in the relationship between  $CC_{gnd}$  and  $CC_{lid}$ . Height to crown center was estimated with slightly greater precision on the 1.5 m plots ( $s_y = 0.68$  m, mean difference =  $-0.25$  m) than on the 2.4 m plots ( $s_y = 0.69$  m, mean difference =  $-0.55$  m) or the 3.0 m plots ( $s_y = 0.75$  m, mean difference =  $-0.62$  m).

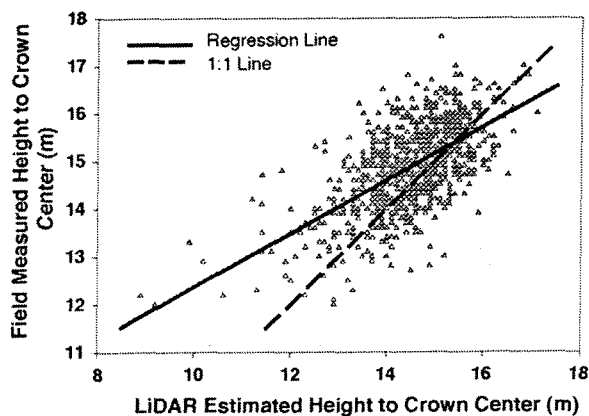


Fig. 3. Field-measured vs. LiDAR-estimated height to crown center for correctly identified trees at the Starr site in Mississippi (regression relationship:  $CC_{gnd} = 6.78 + 0.56CC_{lid}, n = 846, r^2 = 0.40$ ).

The trees at the Fred site were only 4-years-old with crowns extending nearly to the ground. No attempt was made to estimate height to crown center with the Texas data.

### 3.5. Leaf area estimation

Ground-based estimates of leaf area per tree calculated from measurements of DBH and the distance between breast height and crown center (Eq. (1)) for all correctly identified trees on the Starr Forest averaged  $28.4 \text{ m}^2$  with a standard deviation of  $15.9 \text{ m}^2$  (Table 5). Differences between ground-based versus LiDAR-based estimates of leaf area varied with the crown dimension used in the calculation. Individual tree leaf area calculated using LiDAR-based estimates of tree height (after correction for height estimation bias) and crown diameter (Eq. (2)) averaged  $24.7 \text{ m}^2$ , or  $3.6 \text{ m}^2 \text{ tree}^{-1}$  less than the ground-based estimates ( $t_n = 757 = 10.0, P < 0.0001$ ). When LiDAR-estimated distance between breast height and crown center was used in the calculation (Eq. (3)), leaf area was over predicted by an average of  $12.3 \text{ m}^2$  ( $t_n = 750 = 21.0, P < 0.0001$ ). The stronger correlation between leaf areas calculated from Eqs. (1) and (2) versus Eqs. (1) and (3) is reflected in the differences in the regression relationships between leaf areas calculated with these equations:

$$LA_1 = 1.87 + 1.07LA_2$$

$$(r^2 = 0.61, n = 757, s_y = 9.9 \text{ m}^2)$$

$$LA_1 = 8.28 + 0.49LA_3$$

$$(r^2 = 0.44, n = 750, s_y = 11.9 \text{ m}^2)$$

The correlation between  $LA_1$  and  $LA_2$  is stronger and the slope is nearly equal to 1.0 indicating a consistent bias (Fig. 4a). The relationship between  $LA_1$  and  $LA_3$ , with a slope of 0.49, does not suggest such a consistent bias (Fig. 4b).

The average ground-based estimate of leaf area for all live trees at the Starr site was  $24.6 \text{ m}^2$ —about  $3.8 \text{ m}^2$  less than the average leaf area of trees correctly identified with LiDAR (Table 5). Trees missed by LiDAR (omission errors) had a leaf area of only  $12.9 \text{ m}^2$ , again reflecting LiDAR's tendency to fail to detect smaller than average trees.

Table 5

Average leaf area per tree for correctly identified trees, all live trees, all LiDAR identified trees, and omission error and commission error trees at the Starr site (Mississippi) and the Fred site (Texas)

Category	Starr Forest (m <sup>2</sup> )			Fred site (m <sup>2</sup> )	
	Ground	LiDAR		Ground	LiDAR
		CD <sup>a</sup>	CC <sup>b</sup>		
Correct ID trees	28.4 (15.9)	24.7 (11.6)	40.7 (21.3)	14.6 (8.5)	15.0 (8.2)
All trees	24.6 (15.7)			14.8 (8.6)	
All LiDAR trees		23.8 (11.8)	40.4 (22.2)		15.1 (8.3)
Omitted trees	12.9 (7.4)			14.8 (8.6)	
Committed trees		15.1 (10.1)	37.4 (31.2)		15.2 (8.6)

Standard deviations are in parentheses.

<sup>a</sup> Leaf area predicted using LiDAR estimates of crown diameter (Eq. (2)).

<sup>b</sup> Leaf area predicted using LiDAR estimates of height to crown center (Eq. (3)).

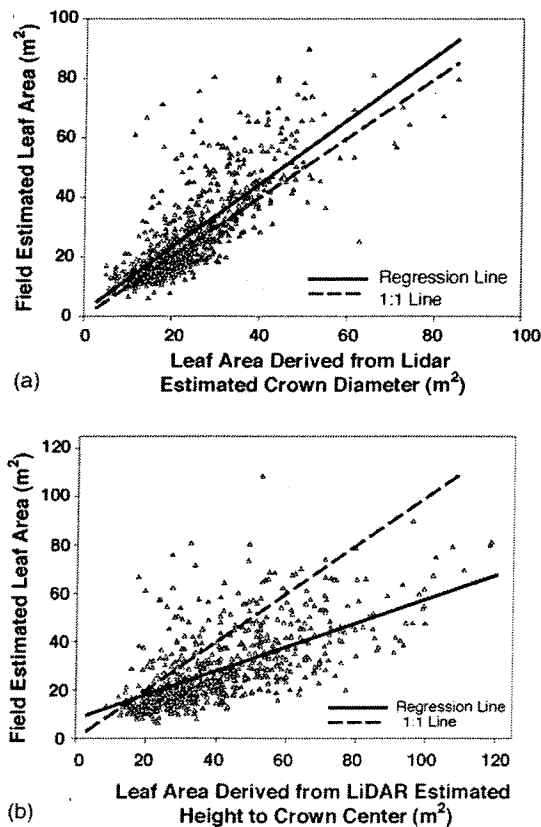


Fig. 4. Ground-based estimates of individual tree leaf area vs. LiDAR-derived leaf area estimates for correctly identified trees at the Starr site in Mississippi. LiDAR estimates derived from (a) LiDAR estimates of crown diameter (regression relationship:  $LA_1 = 1.87 + 1.07 LA_2$ ,  $n = 757$ ,  $r^2 = 0.61$ ) and (b) LiDAR estimates of height to crown center (regression relationship:  $LA_1 = 8.28 + 0.49 LA_3$ ,  $n = 750$ ,  $r^2 = 0.44$ ).

Differences in individual tree leaf area associated with different initial tree spacing were detected by LiDAR-based estimates (Table 6). Leaf area estimated with Eq. (2) averaged 19.0 m<sup>2</sup>, 31.0 m<sup>2</sup> and 37.4 m<sup>2</sup> for trees on the 1.5 m, 2.4 m and 3.0 m plots, respectively (Table 6). The difference between ground- and LiDAR-based leaf area estimates was also affected by initial tree spacing ( $F_{2,39} > 43.7$ ,  $P < 0.001$ ). Calculated with Eq. (2), LiDAR-based estimates of leaf area per tree averaged 0.1 m<sup>2</sup> greater than ground-based estimates of leaf area for trees initially spaced 1.5 m apart. LiDAR-based estimates averaged 5.9 m<sup>2</sup> and 14.5 m<sup>2</sup> less than ground-based estimates for trees initially spaced 2.4 m and 3.0 m apart, respectively. Calculated with Eq. (3), LiDAR-based estimates of leaf area averaged 13.0 m<sup>2</sup>, 13.9 m<sup>2</sup> and 8.2 m<sup>2</sup> greater than ground-based estimates for trees initially spaced at 1.5 m, 2.4 m and 3.0 m, respectively (Table 6).

At the Fred site, mean leaf area calculated from ground measurements of tree height was 14.6 m<sup>2</sup> for trees correctly identified with LiDAR. The average LiDAR-based leaf area, calculated from LiDAR estimates of tree height, was 15.0 m<sup>2</sup>, resulting in an average difference from ground-based estimates of 0.4 m<sup>2</sup>. This difference, however, does not represent a consistent bias since the slope of the relationship between the two estimates is not close to 1.0 ( $LA_{\text{gnd}} = 9.75 + 0.324 LA_{\text{lid}}$ ;  $r^2 = 0.098$ ,  $n = 1269$ ,  $P < 0.001$ ). The mean difference between ground- and LiDAR-based estimates of leaf area per tree was not affected by any of the regeneration practices used in this study ( $F_{1,14} < 1.9$ ,  $P > 0.193$ ).

Table 6

Initial tree spacing effects on ground- and LiDAR-based estimates of average individual tree leaf area, and the difference between ground- and LiDAR-based leaf area estimates, for trees correctly identified using LiDAR at the Starr site (Mississippi)

Initial tree spacing	Ground (m <sup>2</sup> )	LiDAR <sup>a</sup> (m <sup>2</sup> )	Difference (m <sup>2</sup> )	LiDAR <sup>b</sup> (m <sup>2</sup> )	Difference (m <sup>2</sup> )
	LA <sub>1</sub>	LA <sub>2</sub>	LA <sub>2</sub> – LA <sub>1</sub>	LA <sub>3</sub>	LA <sub>3</sub> – LA <sub>1</sub>
1.5 m × 1.5 m	18.9	19.0	0.1	31.8	13.0
2.4 m × 2.4 m	36.9	31.0	–5.9	50.8	13.9
3.0 m × 3.0 m	51.9	37.4	–14.5	60.1	8.2

<sup>a</sup> Leaf area predicted using LiDAR estimates of crown diameter ( $LA_2 = 0.0068HT^{2.7993}CD^{0.4405}$ ).

<sup>b</sup> Leaf area predicted using LiDAR estimates of height to crown center ( $LA_3 = 0.0007 HT^{7.1342}/HT_{mc}^{3.8145}$ ).

#### 4. Discussion

LiDAR-based approaches based on direct estimation of individual tree structural parameters have advantages over statistical approaches that use multiple regression techniques to draw correlations between mean stand parameters and statistical metrics derived from the LiDAR data. While correlations developed under regression approaches, in some instances, have been relatively strong, they require the development of new correlations for each set of unique stand conditions, thus limiting their utility. Individual tree approaches, such as presented here, have the potential to develop into a set of tools applicable over a wide range of stand types and conditions. Individual tree leaf area estimation equations would still need to be developed. However, as with more conventional allometric-based relationships, these equations would likely be relatively robust, particularly across a well-defined range of conditions (e.g., Long and Smith, 1988). Therefore, new equations would not need to be developed for each LiDAR data set.

##### 4.1. Tree identification accuracy

Accurate identification of trees is critical if individual tree values are going to be aggregated to stand-level means and totals. Correct identification of live trees using LiDAR at the Starr site averaged 81%, ranging from 68% on the higher density plots to 93% on the lower density plots. When identification errors (both omission and commission) were factored in, net identification accuracy using LiDAR averaged 89%, ranging from about 33% underestimation on the higher density plots to about 3% overestimation on the low density plots. Omission error trees, those that

LiDAR failed to detect, tended to be smaller than average trees at the Starr site. Commission error trees, peaks in the canopy layer identified as trees when no live pine tree currently existed, also tended to be smaller than average.

At the Fred site, correct identification averaged 70%, while net accuracy averaged nearly 88%. There were no systematic differences in the average size of correctly identified trees and that of the omission or commission error trees. One problem encountered at the Fred site was that given the small stature of the trees, and the fact that the canopy had not yet reached closure, there was an abundance of competing vegetation on many of the plots. The competing vegetation often consisted of woody shrubs that were as tall or taller than the target loblolly pine. As a result, even when a tree was apparently identified correctly, there was some uncertainty in whether the peak in the LiDAR canopy surface was associated with the target pine or from competing vegetation. Another consequence of the competing vegetation was that the Fred site had a much greater commission error rate (17.7%) than the Starr site (8.0%).

The results of our analysis compare favorably with other studies that have attempted to estimate stem density using LiDAR. McCombs et al. (2003), using a different LiDAR data set collected at the Starr site, reported net accuracy ranging from 67% on the 2.4 m plots to 93% on the 3.0 m plots. They were unable to successfully identify trees in the 1.5 m plots. Young et al. (2000) reported density estimates in 9–16-year-old loblolly pine plantations ranging from 5% underestimation to 12% overestimation, with an average absolute error of 5%. Reexamination of their data, however, indicates that both commission and omission error rates were higher than the net accuracy would suggest. Using a multiple regression correlation

approach between stem density and various canopy height and density metrics derived from LiDAR data, Næsset (2002) was able to explain only 50–68% of the variation in stem density in mature Norway spruce and Scots pine stands. The standard deviation of the differences between predicted and observed values ranged from 17% to 22% or 128–440 stems  $\text{ha}^{-1}$ .

Our ability to accurately detect trees at the Fred site was somewhat lower, likely because of smaller tree sizes, lack of crown closure and abundant competing vegetation. Other studies have also had difficulties in estimating stem densities in younger stands. For example, in Norway spruce and Scots pine stands with heights less than 6 m, Næsset and Bjerknes (2001) could explain only 42% of the variation in stem density, and the standard deviation of the differences between predicted and observed values was 29% or 1209 stems  $\text{ha}^{-1}$ .

#### 4.2. Height measurement

Underestimation of tree heights is commonly observed in LiDAR studies that attempt direct estimates of either individual tree heights (Magnussen and Boudewyn, 1998; McCombs et al., 2003) or stand average heights (Nilsson, 1996; Næsset, 1997a; Magnussen et al., 1999). The cause of this underestimation has often been attributed to LiDAR footprints striking the sides of crowns and missing the apex of most trees (Magnussen and Boudewyn, 1998). With posting densities ranging from  $4 \text{ m}^{-2}$  to  $20 \text{ m}^{-2}$  and a footprint size of ca. 0.11 m, the LiDAR ground coverage for our study was generally between 5% and 15%, suggesting that our canopy returns very often were generated from somewhere below the terminal leader of a tree. Even if a LiDAR post does strike the top of a tree crown; however, it may not reflect enough energy to generate a measurable return until the footprint of energy has traveled some vertical distance down the crown, an effect called range averaging (Lefsky et al., 2002).

LiDAR-based height estimation errors for correctly identified individual trees at the Starr site ranged from  $-3.6 \text{ m}$  to  $+2.5 \text{ m}$ , averaging  $-0.5 \text{ m}$ . Regression analysis resulted in an intercept of 0.5 and a slope of nearly 1.0, suggesting that the underestimation represented a consistent bias unrelated to initial spacing and current growing conditions.

At the Fred site, while the standard deviation of the LiDAR height estimates was nearly identical to that of the Starr site, the LiDAR height estimation errors ranged from  $-4.0$  to  $+5.8$  and the correlation between ground and LiDAR heights was weak. Problems associated with small target trees and competing vegetation that hampered tree identification also appear to have caused difficulty in consistently estimating tree heights accurately. LiDAR overestimated individual tree heights at Fred by an average of only 0.2 m but regression analysis did not suggest a consistent bias. Rather, errors at the Fred site appeared random. A consistent bias is easily adjusted for, but does require the extra step of determining the bias specific to a given set of stand conditions, species and LiDAR posting density. One approach to addressing bias correction may be to incorporate LiDAR into a double-sampling scheme that includes a minimum amount of field data for calibrating the LiDAR estimates (Parker and Evans, 2004).

McCombs et al. (2003), working with the two wider spacings from the Starr site, also found a bias of approximately  $-0.5 \text{ m}$ , again unrelated to spacing and growing conditions. Lim et al. (2001), working in hardwood forests, were able to achieve a near one-to-one correspondence between LiDAR heights and measured heights by manually locating and measuring heights from the canopy surface model. The difference in precision may stem from the broad crown architecture of hardwoods compared to the more conical crowns of conifers.

#### 4.3. Crown dimensions

Deriving physical crown dimensions using LiDAR was difficult. Crown diameter, in particular, is inherently difficult to estimate, whether remotely or from the ground. Individual crown diameters of correctly identified trees at the Starr site were underestimated by an average of 15–20% (Table 4), with errors ranging from  $-3.5 \text{ m}$  to  $+2.4 \text{ m}$ . At the Fred site, we were unable to generate useful estimates of crown diameter from the LiDAR data. At 4 years of age, these plots had not yet reached canopy closure. Given the techniques used to identify crown edges, the saddles occurring between adjacent peaks in the interpolated canopy surface simply split the distance

between trees, thus greatly overestimating crown diameters.

A problem in estimating crown diameter is that crowns are commonly assumed circular in cross-section. In reality, crowns tend to be asymmetrical with irregular edges, even in regularly spaced plantations. The technique employed in this study measured the distance from a crown peak in the interpolated canopy surface model to the perceived crown edge in each of four cardinal directions. Precisely identifying the location of the crown edge was difficult, however. Both approaches attempted tended to underestimate crown widths. Given the irregular nature of crowns, better results may have been attained by measuring more than four crown radii.

Compounding the errors inherent in our analytical approach, the measurement of crown diameter in the field is also difficult. Field procedures tend to measure to an imaginary crown edge that connects the tips of the longest branches, or the tips of branches that may not have enough biomass to generate a LiDAR return. Field measurements may not be taken at exact cardinal directions, but rather measure to the end of the longest branches. LiDAR is more likely to estimate the edge of the crown as defined by the predominance of crown biomass, not the absolute extent of the longest branch. In a detailed study modeling crown shape in loblolly pine, Baldwin et al. (1997) also found that prediction models underestimated crown diameter.

Our LiDAR-based estimates of height to crown center of individual trees at the Starr site were more precise than our estimates of crown diameter. Average estimation error was less than 3% of the average field measured height to crown center, ranging from  $-3.4$  m to  $+2.2$  m. At the Fred site, however, LiDAR was unable to provide useful estimates of height to crown center. Again, canopy closure had not yet occurred nor had crown recession progressed noticeably. Without inter-crown contact, our approach was unable to provide useful information on height to crown center. In plantations of this age, however, estimates of height to crown center will likely be less important or can simply be assumed to be one-half of tree height.

#### 4.4. Leaf area estimates

The potential feasibility of using tree dimensions obtained from airborne sensors to estimate leaf area

was demonstrated by Roberts et al. (2003). They found that estimates of individual tree leaf area derived from measures of tree height and crown structural dimensions were as precise as leaf area predicted from DBH. They also reported that the most precise predictions were obtained when both vertical and horizontal crown dimensions were included in prediction equations. In developing the leaf area prediction equations for the trees at the Starr Forest, a model with tree height, crown diameter and distance from breast height to crown center did not improve the precision in calculating leaf area over either Eqs. (2) or (3). At the Fred site, leaf area was estimated from tree height alone since crown diameter could not be reliably determined from the LiDAR data.

The underestimation of individual tree leaf area calculated with Eq. (2) relative to leaf area calculated with Eq. (1) reflects the underestimation of crown diameter. Conversely, because individual tree leaf area is inversely related to the distance between breast height and crown center, LiDAR underestimation of height to crown center caused an overestimation of leaf area using Eq. (3). LiDAR-based estimation errors for crown diameter exceeded estimation errors for height to crown center by ca. 0.3 m; however, the errors in estimating leaf area with Eq. (2) were considerably less, on average, than when estimating leaf area with Eq. (3) ( $-5.2\%$  versus  $58\%$ , respectively). The sensitivity of leaf area estimates to errors in crown dimensions can be evaluated from the fitted exponents for the two crown variables. The exponent for crown diameter in Eq. (2) is 1.911, while the exponent for height to crown center in Eq. (3) is  $-2.91$ . A 10% underestimation of height to crown center increases predicted leaf area by a factor of 1.5, while a 10% underestimation of crown diameter decreases predicted leaf area by a factor of only 0.8.

The effect of initial spacing on prediction errors in individual tree leaf area at the Starr site is linked to the errors in measuring crown diameter and height to crown center, and the propagation of these errors through the prediction equations. LiDAR-based estimates of crown diameter and height to crown center were closer to ground-measured values for trees at tighter spacings, and thus, LiDAR-based leaf area estimates for trees on the 1.5 m plots were closer to ground-based estimates than on the lower density plots.

At the Fred site, since leaf area per tree is estimated solely as a function of tree height, the success in predicting leaf area depends exclusively on the ability of LiDAR to estimate tree height. LiDAR-based estimates of height at Fred differed little, on average, from ground measured heights, and the ability to estimate height with LiDAR was not affected by any of the treatments. Therefore, our LiDAR-based estimates of leaf area for accurately identified trees were, on average, very close to ground-based estimates of leaf area.

## 5. Conclusions

Initial tree spacing significantly affected the ability of LiDAR to estimate several tree and stand parameters. Thus, knowledge of approximate tree spacing prior to LiDAR analysis is important for setting appropriate focal filter sizes for tree identification and height determination. However, spacing is a design parameter in most plantations and is often verified after planting, which would provide needed density information. Other studies have developed approaches that automatically set filter size without relying on prior stand information (Popescu et al., 2003; Popescu and Wynne, 2004). Thus, individual tree-based LiDAR approaches appear capable of providing reliable estimates of stem density and tree heights in loblolly pine plantations similar to those examined in this study. Refinement of existing approaches or development of new approaches to approximate stem density prior to setting filter sizes for tree finding algorithms would facilitate the use of LiDAR in natural stands with greater spatial variation in tree spacing.

The most limiting factor in this study was the ability of the techniques we used to reliably estimate crown diameter and vertical crown dimensions such as height to crown center or height to crown base. Development of better analytical tools for using LiDAR data to estimate crown dimensions is certainly possible, and will be required before suitably precise estimates of individual tree leaf area, and thus, stand-level estimates of leaf area index can be provided. Approaches based on correlating the vertical distribution of LiDAR canopy returns with the vertical distribution of crown biomass have shown promise

(Magnussen and Boudewyn, 1998; Jerez et al., 2005). Incorporation of high-resolution spectral imagery may also prove useful in estimating horizontal crown dimensions.

LiDAR-based individual tree analytical techniques are currently capable of providing suitably precise estimates of stand density and average stand height for operational use in inventories of southern pine plantations. Additional research is needed to develop tools that use LiDAR, alone or in conjunction with other remote sensing technologies, to provide suitably precise estimates of crown dimensions. Crown dimension estimates can then be used to estimate leaf area, stem diameters and stem volumes. The continued development of analytical approaches incorporating the use of LiDAR data appears likely, as does the increased use of this technology in forest management operations.

## Acknowledgements

The authors would like to express appreciation to Dr. Robert Parker and Mr. Curtis Collins for helpful comments on an earlier draft of this paper. This research was supported by NASA grant NAG13-99018. Approved for publication as Journal Article No. FO-271 of the Forest and Wildlife Research Center, Mississippi State University.

## References

- Andersen, H.-E., Reutebuch, S.E., Schreuder, G.F., 2001. Automated individual tree measurement through morphological analysis of a LiDAR-based canopy surface model. In: Proceedings of the First International Precision Forestry Cooperative Symposium, Institute of Forest Resources, University of Washington, Seattle, WA, 17–20 June, pp. 11–22.
- Baldwin Jr., V.C., Peterson, K.D., Burkhart, H.E., Amateis, R.L., Dougherty, P.M., 1997. Equations for estimating loblolly pine branch and foliage weight and surface area distributions. *Can. J. Forest Res.* 27, 918–927.
- Carter, M.C., Dean, T.J., Zhou, M., Messina, M.G., Wang, Z., 2002. Short-term changes in soil C, N, and biota following harvesting and regeneration of loblolly pine (*Pinus taeda* L.). *Forest Ecol. Manage.* 164, 67–88.
- Dean, T.J., Roberts, S.D., Gilmore, D.W., Maguire, D.A., O'Hara, K.L., Seymour, R., Long, J.N., 2002. An evaluation of the uniform stress hypothesis based on stem taper in conifer stems. *TREES* 16, 559–568.

- Fassnacht, K.S., Gower, S.T., Norman, J.M., McMurtrie, R.E., 1994. A comparison of optical and direct methods for estimating foliage surface area index in forests. *Agric. Forest Meteorol.* 71, 183–207.
- Fassnacht, K.S., Gower, S.T., MacKenzie, M.D., Nordheim, E.V., Lillesand, T.M., 1997. Estimating the leaf area index of north central Wisconsin forests using the Landsat Thematic Mapper. *Remote Sens. Environ.* 61, 229–245.
- Gower, S.T., Norman, J.M., 1991. Rapid estimation of leaf area index in conifer and broad-leaf plantations. *Ecology* 72, 1896–1900.
- Gower, S.T., Vogt, K.A., Grier, C.C., 1992. Carbon dynamics of rocky mountain Douglas-fir—influence of water and nutrient availability. *Ecol. Monogr.* 62, 43–65.
- Hall, S.A., Burke, I.C., Box, D.O., Kaufmann, M.R., Stoker, J.M., 2005. Estimating stand structure using discrete-return LiDAR: an example from low density, fire prone ponderosa pine forests. *Forest Ecol. Manage.* 208, 189–209.
- Holmgren, P., Thuresson, T., 1998. Satellite remote sensing for forestry planning—a review. *Scand. J. Forest Res.* 13, 90–110.
- Hyypä, J., Inkinen, M., 1999. Detecting and estimating attributes for single trees using laser scanner. *Photogramm. J. Finland* 16, 27–42.
- Hyypä, J., Kelle, O., Lehikinen, M., Inkinen, M., 2001. A segmentation-based method to retrieve stem volume estimates from 3-D tree height models produced by laser scanners. *IEEE Trans. Geosci. Remote Sens.* 39, 969–975.
- Jerez, M., Dean, T.J., Cao, Q.V., Roberts, S.D., 2005. Describing leaf area distribution in loblolly pine trees with Johnson's SB function. *Forest Sci.* 51, 93–101.
- Lefsky, M.A., Cohen, W.B., Parker, G.G., Harding, D.J., 2002. LiDAR remote sensing for ecosystem studies. *Bioscience* 52, 19–30.
- Lim, K., Treitz, P., Groot, A., St-Onge, B., 2001. Estimation of individual tree heights using LiDAR remote sensing. In: *Proceedings of the 23rd Canadian Symposium on Remote Sensing, Quebec, Que. CASI, Ottawa, Ont. 21–24 August*, pp. 243–250.
- Land Jr., S.B., Belli, K.L., Duzan Jr., H.W., 1991. Family, spacing, and family-by-spacing effects on loblolly pine during five years after planting. In: *Coleman, S.S., Neary, D.G. (Compilers), Proceedings Sixth Biennial Southern Silviculture Research Conference. USDA Forest Service. Gen. Tech. Re SE-70*, pp. 744–756.
- Long, J.N., Smith, F.W., 1988. Leaf area–sapwood area relations of lodgepole pine as influenced by stand density and site index. *Can. J. Forest Res.* 18, 247–250.
- Magnussen, S., Boudewyn, P., 1998. Derivations of stand heights from airborne laser scanner data with canopy-based quantile estimators. *Can. J. Forest Res.* 28, 1016–1031.
- Magnussen, S., Effermont, P., LaRiccia, V.N., 1999. Recovering tree heights from airborne laser scanner data. *Forest Sci.* 45, 407–422.
- McCombs, J.W., Roberts, S.D., Evans, D.L., 2003. Influence of fusing LiDAR and multispectral imagery on remotely sensed estimates of stand density and mean tree height. *Forest Sci.* 49, 457–466.
- McCrary, R.L., Jokela, E.J., 1998. Growth phenology and crown structure of selected loblolly pine families planted at two spacings. *Forest Sci.* 42, 46–57.
- Means, J.E., Acker, S.A., Fitt, B.J., Renslow, M., Emerson, L., Hendrix, C.J., 2000. Predicting forest stand characteristics with airborne scanning LiDAR. *Photogramm. Eng. Remote Sens.* 66, 1367–1371.
- Næsset, E., 1997a. Determination of mean tree height of forest stands using airborne laser scanner data. *ISPRS J. Photogramm. Remote Sens.* 52, 49–56.
- Næsset, E., 1997b. Estimating timber volume of forest stands using airborne laser scanner data. *Remote Sens. Environ.* 61, 246–253.
- Næsset, E., 2002. Predicting forest stand characteristics with airborne scanning laser using a practical two-stage procedure and field data. *Remote Sens. Environ.* 80, 88–99.
- Næsset, E., Bjercknes, K.-O., 2001. Estimating tree heights and number of stems in young forest stands using airborne laser scanner data. *Remote Sens. Environ.* 78, 328–340.
- Næsset, E., Økland, T., 2002. Estimating tree height and tree crown properties using airborne scanning laser in a boreal nature reserve. *Remote Sens. Environ.* 79, 105–115.
- Nilsson, M., 1996. Estimation of tree heights and stand volume using an airborne LiDAR system. *Remote Sens. Environ.* 56, 1–7.
- Parker, R.C., Evans, D.L., 2004. An application of LiDAR in a double-sample forest inventory. *West. J. Appl. Forest* 19, 95–101.
- Popescu, S.C., Wynne, R.H., 2004. Seeing the trees in the forest: using LiDAR and multispectral data fusion with local filtering and variable window size for estimating tree height. *Photogramm. Eng. Remote Sens.* 70, 589–604.
- Popescu, S.C., Wynne, R.H., Nelson, R.F., 2003. Using LiDAR for measuring individual trees in the forest: an algorithm for estimating the crown diameter. *Can. J. Remote Sens.* 29, 564–577.
- Popescu, S.C., Wynne, R.H., Scriver, J.A., 2004. Fusion of small-footprint LiDAR and multispectral data to estimate plot-level volume and biomass in deciduous and pine forests in VA, USA. *Forest Sci.* 50, 551–565.
- Roberts, S.D., Dean, T.J., Evans, D.L., 2003. Family influences on leaf area estimates derived from crown and tree dimensions in *Pinus taeda*. *Forest Ecol. Manage.* 172, 261–270.
- Shelburne, V.B., Hedden, R.L., Allen, R.M., 1993. The effects of site, stand density, and sapwood permeability on the relationship between leaf area and sapwood area in loblolly pine (*Pinus taeda* L.). *Forest Ecol. Manage.* 58, 193–209.
- Sinclair, T.R., Knoerr, K.R., 1982. Distribution of photosynthetically active radiation in the canopy of a loblolly pine plantation. *J. Appl. Ecol.* 19, 183–191.
- Spanner, M., Johnson, L., Miller, J., McCreight, R., Freemantle, J., Runyon, J., Gong, P., 1994. Remote sensing of seasonal leaf area index across the Oregon transect. *Ecol. Appl.* 4, 258–271.
- Whitehead, D., 1978. The estimation of foliage area from sapwood basal area in Scots pine. *Forestry* 51, 137–149.
- Wu, Y., Strahler, A.H., 1994. Remote estimation of crown size, stand density, and biomass on the Oregon transect. *Ecol. Appl.* 4, 299–312.
- Wulder, M.A., Franklin, S.E., Lavigne, M.B., 1996. High spatial resolution optical image texture for improved estimation of

- forest stand leaf area index. *Can. J. Remote Sens.* 22, 441–449.
- Wulder, M.A., LeDrew, E.F., Franklin, S.E., Lavigne, M.B., 1998. Aerial image texture information in the estimation of northern deciduous and mixed wood forest leaf area index (LAI). *Remote Sens. Environ.* 64, 64–76.
- Young, B., Evans, D.L., Parker, R.C., 10–12 January 2000. Methods for comparison of LIDAR and field measurements of loblolly pine. In: *Proceedings of the Second International Conference on Geospatial Information in Agriculture and Forestry*, Lake Buena Vista, FL, . ERIM International, pp. 193–199.
-

